

# Advanced 18 nm Quad-MTJ technology overcomes dilemma of Retention and Endurance under Scaling beyond 2X nm

H. Naganuma,<sup>1,2,3</sup> S. Miura,<sup>1</sup> H. Honjo,<sup>1</sup> K. Nishioka,<sup>1</sup> T. Watanabe,<sup>1</sup> T. Nasuno,<sup>1</sup> H. Inoue,<sup>1</sup>

T. V. A. Nguyen,<sup>2,3</sup> Y. Endo,<sup>4</sup> Y. Noguchi,<sup>1</sup> M. Yasuhira,<sup>1</sup> S. Ikeda,<sup>1,2,3,5</sup> and T. Endoh<sup>1-5</sup>

<sup>1</sup>Center for Innovative Integrated Electronic Systems, Tohoku Univ., Sendai 980-0845, Japan, <sup>2</sup>Center for Science and Innovation in Spintronics, Tohoku Univ., <sup>3</sup>Center for Spintronics Research Network, Tohoku Univ., <sup>4</sup>Graduate School of Engineering, Tohoku Univ. <sup>5</sup>Research Institute of Electrical Communication, Tohoku Univ.

## Abstract

Advanced quad-interfaces perpendicular magnetic tunnel junction (Quad-MTJ) was developed by engineering a low effective damping constant ( $\alpha_{\text{eff}}$ ) material in free layer with high perpendicular magnetic anisotropy (PMA), and low resistance area product ( $RA$ ) in MgO layers, and stable reference layer. The advanced 18 nm Quad-MTJ fabricated by the developed low-damage 300 mm fabrication process exhibited following performances over those of Double-MTJ; (a) 1.77 times larger thermal stability factor ( $\Delta$ ), (b) 0.83 times smaller writing current ( $I_c$ ) at 10 ns, (c) 2.1 times higher write efficiency ( $\Delta/I_c$ ) at 10 ns. Thanks to the above excellent MTJ stack design, it is the first time beyond 2X nm generation that the advanced 18 nm Quad-MTJ achieves at least  $6 \times 10^{11}$  endurance with 10 years retention. Consequently, the advanced Quad-MTJ technologies have broken out the dilemma issue of retention and endurance even under scaling of 2X nm.

**Keywords:** 1X nm, STT-MRAM, p-MTJ, quad interface

## Introduction

STT-MRAM has dilemma between retention and endurance due to opposite effect of  $\Delta$  and endurance on PMA. Scaling down MTJ degrades this trade-off, especially beyond 2X nm. The shape anisotropy MTJ has been demonstrated in principle for an advantage for scaling in  $\Delta$  by large shape-PMA [1,2], however has not yet verified other performances under practical usage condition. Therefore, a CoFeB/MgO based i-PMA p-MTJ including Quad-MTJ [3-6] keep a promising technology position and is required higher performance. In order to obtain enough endurance in scaling, low resistance product ( $RA$ ) in MgO layers and low damping constant ( $\alpha_{\text{eff}}$ ) in free layer are essential, because these are linear relation to writing voltage ( $V_c$ ). In this study, the advanced MTJ stack for Quad-MTJ was designed and its excellent performance were successfully demonstrated at 18 nm technology.

### Advanced Quad-MTJ with low damage 300 mm process

The advanced Quad-MTJ stacks with low  $\alpha_{\text{eff}}$  free, low  $RA$  MgO, and stable reference layers were developed (Fig.1). The advanced Quad-MTJs patterned from 48 nm to 11 nm were successfully fabricated after annealing at 400°C (Fig.2). Three and two MgO layers were clearly observed, and no re-deposition at side wall was confirmed owing to advanced low-damage integration process (PVD, Etching, etc.). The advanced Quad-MTJ showed approximately half  $\alpha_{\text{eff}}$  and twice PMA of Double-MTJ (Fig.3) together with a low  $RA \sim 2 \Omega/\mu\text{m}^2$ . The large exchange coupling ( $H_{\text{exc}}$ ) in reference layer of more than 0.7 T was achieved by developed reference layer (Fig.4).

### Demonstration of 1X nm Quad-MTJ

#### A. TMR ratio vs. CD

Over 100% TMR ratio, zero-shift magnetic field, and stable reference layer against external magnetic field ( $H_{\text{ext}}$ ) were realized down to 11 nm advanced Quad-MTJ with developing novel free, MgO, and reference layer (Fig.4, 5). The TMR ratio vs. CD showed almost constant owing to minimize damaged

sidewall layer thanks to the low-damage process (Fig. 5).

#### B. Thermal stability $\Delta$ vs. CD

Figure 6 shows (a) the  $R$ - $H$  curves measured 100 times for the advanced 18 nm Quad-MTJ, and (b)  $\Delta$  vs. CD for the advanced Quad- and Double MTJs down to 11 nm. Blank circles and solid circles/squares represent  $\Delta$  evaluated by the pulse magnetic field and current.  $\Delta$  values obtained from the two different methods are in good agreement. The advanced 18 nm Quad-MTJ shows the 1.8 times larger  $\Delta$  compared with the Double-MTJ thanks to twice the number of i-PMA interfaces.

#### C. Write error rate (WER) vs. write voltage

The advanced 18 nm Quad-MTJ achieved small writing current at high-speed of 10 ns (Fig. 7). Because the advanced Quad-MTJ employed stable reference layer (Fig. 4), the back-hopping due to undesirable reference layer flip was not observed even with WER of  $10^{-6}$ . Furthermore, the advanced 18 nm Quad-MTJ has sharp WER curves at small  $t_w$  by a large number of i-PMA layers.

#### D. Switching phase diagram (SFD) under magnetic field

SFD at parallel (P) to antiparallel (AP) switching (write '1') as a function of  $H_{\text{ext}}$ , and bias voltage ( $V$ ) was carried out at  $t_w = 20$  and 200 ns (Fig. 8). The influence of  $H_{\text{ext}}$  on switching boundaries was small in the advanced 18 nm Quad-MTJ due to its large i-PMA. No back-hopping behavior and no ballooning of switch boundary was occurred in SFD thanks to the developed reference layer of the advanced 18 nm Quad-MTJ.

#### E. Writing current $I_c$ vs. Pulse width $t_w$

From  $t_w$  dependence of  $I_c$ ,  $I_c$  of for the advanced 18 nm Quad-MTJ at  $t_w$  of 10 ns has 0.8 times smaller than that of the Double-MTJ (Fig.9); which could be related to low  $\alpha_{\text{eff}}$  and large  $\Delta$  (Fig. 3). Writing efficiency  $\Delta/I_c$  (@10 ns) in the advanced 18 nm Quad-MTJ shows 2.1 times higher owing to large  $\Delta$  and small  $I_c$  in the Quad-MTJ.

#### F. Enough-Endurance in advanced Quad-MTJ

The advanced 18 nm Quad-MTJ achieves at least  $6 \times 10^{11}$  endurance (Fig.10) with 10 years retention thanks to its higher write efficiency.

## Summary

The advanced 18 nm Quad-MTJ (low  $\alpha_{\text{eff}}$  material with high PMA of free layer, low  $RA$  MgO layers, stable reference) employed by novel low-damage 300 mm fabrication process overcomes dilemma of retention and endurance under scaling beyond 2X nm (Fig.11). This technology will contribute to 1X nm STT-MRAM available for wide application from SRAM/eDRAM to eFlash, etc.

## References

- [1] K. Watanabe et al., Nat. Com., **9**, 663 (2018). [2] N. Perrissin, et al, Nanoscale **10**, 12187 (2018). [3] S. Ikeda et al., Nat. Mater. **9**, 721 (2010). [4] T. Saito et al., IEEE Trans. Magn. **54**, 3400505 (2018). [5] K. Nishioka, et al., VLSI (2019). [6] S. Miura et al, IEEE T-ED **67**, 5368 (2020).

**Acknowledgements** This work was supported by CIES's Industrial Affiliation on STT MRAM program and JST-OPERA.

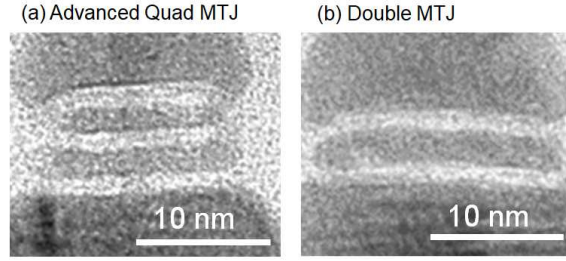
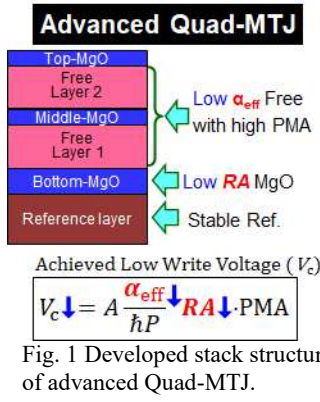


Fig. 2. TEM photographs of advanced 18 nm Quad- and 19 nm Double-MTJs fabricated through our developed low-damage process. A clear stacking structure and etching profile were confirmed.

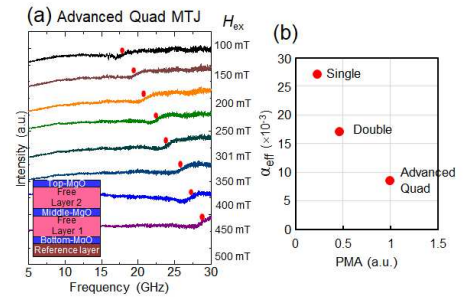


Fig. 3 (a) FMR spectrum of advanced Quad-stack film, and (b) effective damping constant ( $\alpha_{\text{eff}}$ ) vs. PMA for Single, [3] Double, and advanced Quad-stack films.

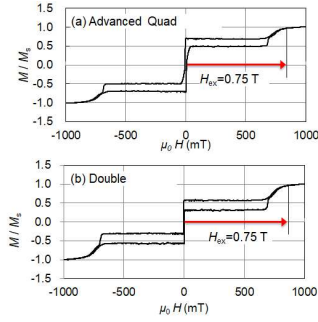


Fig. 4 Magnetization curves of (a) the advanced Quad- and (b) Double-MTJ stack films with novel reference layer.

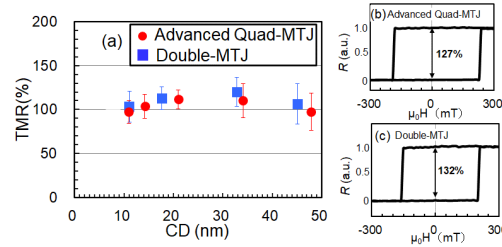


Fig. 5 (a) CD dependence (from 48 nm to 11 nm) of TMR ratio for the advanced Quad- and Double-MTJs. TMR ratio was almost constant with a decrease in the CD.  $R$ - $H$  curves for the (b) advanced Quad- and (c) Double-MTJs. The bi-stable magnetic switching up to 300 mT and almost zero-shift magnetic field was obtained.

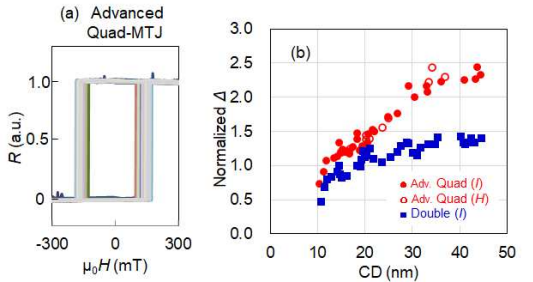


Fig. 6 (a) One hundred  $R$ - $H$  curves for the advanced 18 nm Quad-MTJ, and (b) thermal stability factor  $\Delta$  as a function of CD for the advanced Quad- and Double-MTJs.  $\Delta$ s of the advanced Quad-MTJs are almost 1.77–1.83 times larger than those of the Double-MTJs.

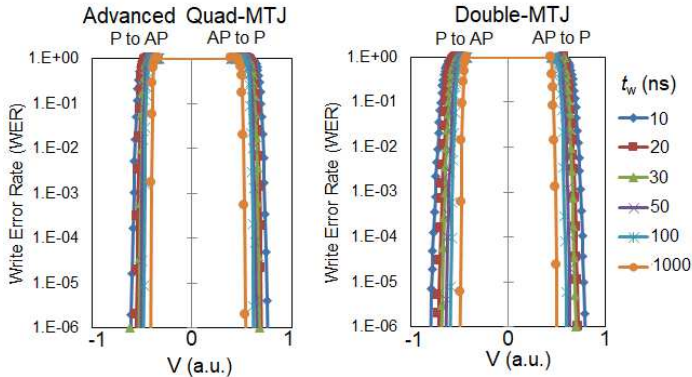


Fig. 7 Write pulse width ( $t_w$ ) dependence of write error rate (WER) at different write voltage for the advanced 18 nm Quad- and Double-MTJs.

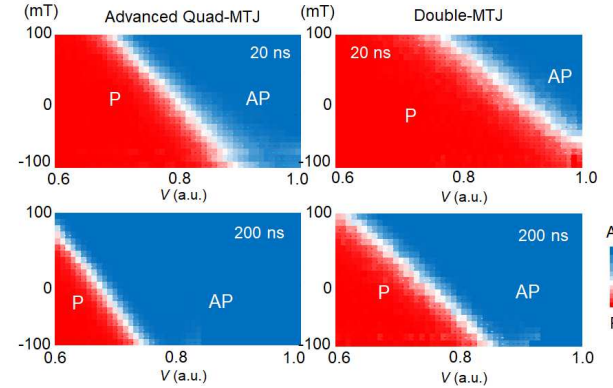


Fig. 8 Switching phase diagram (SPD) as a function of external field ( $H_{\text{ext}}$ ) and bias voltage ( $V$ ) for the advanced 18 nm Quad-MTJ and Double-MTJs. Switching direction of SPD measurement is P to AP.

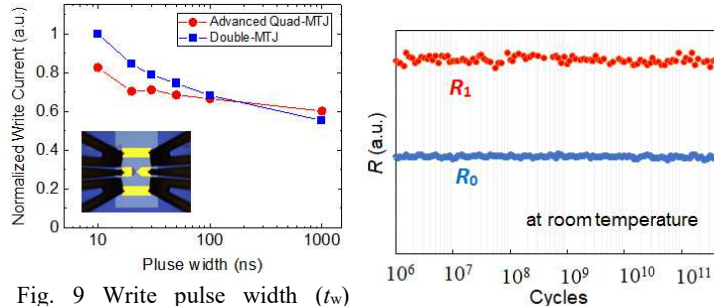


Fig. 9 Write pulse width ( $t_w$ ) dependence of critical writing current ( $I_c$ ) for the advanced 18 nm Quad- and Double-MTJs deduced from WER (Fig. 7). The high-speed measurement was carried out by using co-planar waveguide shown in inset.

Fig. 10 Endurance of the advanced 18 nm Quad-MTJ. Although the Quad-MTJ enhances  $\Delta$ , its endurance exceeds at least  $6 \times 10^{11}$  owing to the low  $RA$  MgO layers and low  $\alpha_{\text{eff}}$ .

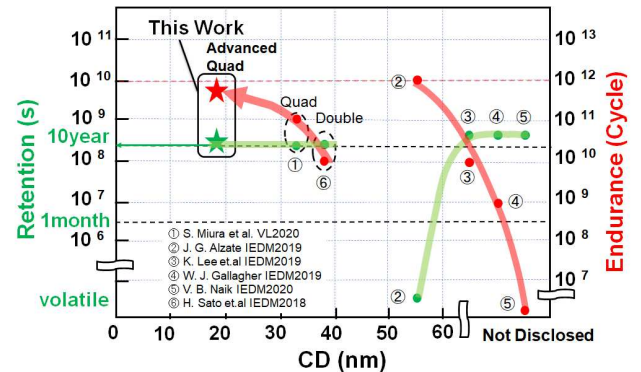


Fig. 11 The retention and endurance vs. CD. Scaling-down makes the dilemma of retention and endurance more severe. The advanced Quad-MTJ enable us to realized overcome the dilemma issue beyond 2X nm.